

Article

Impact of Fe₃O₄, CuO and Al₂O₃ on the AC Breakdown Voltage of Palm Oil and Coconut Oil in the Presence of CTAB

Nur Aqilah Mohamad ^{1,*}, Norhafiz Azis ^{1,2,*}, Jasronita Jasni ¹,
Mohd Zainal Abidin Ab Kadir ^{1,3} , Robiah Yunus ⁴ and Zaini Yaakub ⁵

¹ Advanced Lightning, Power and Energy Research Centre (ALPER), Department of Electrical and Electronic Engineering, Universiti Putra Malaysia, 43400 Serdang, Selangor, Malaysia; jas@upm.edu.my (J.J.); mzk@upm.edu.my (M.Z.A.A.K.)

² Institute of Advanced Technology (ITMA), Universiti Putra Malaysia, 43400 Serdang, Selangor, Malaysia

³ Institute of Power Engineering (IPE), Universiti Tenaga Nasional, 43000 Kajang, Selangor, Malaysia

⁴ Department of Chemical and Environmental Engineering, Faculty of Engineering, Universiti Putra Malaysia, 43400 Serdang, Selangor, Malaysia; robiah@upm.edu.my

⁵ Hyrax Oil Sdn. Bhd., Lot 4937 Batu 51/2, Jalan Meru, Mukim Kapar, 41050 Klang, Selangor, Malaysia; zaini@hyraxoil.com

* Correspondence: qieylaqilah@gmail.com (N.A.M.); norhafiz@upm.edu.my (N.A.)

Received: 8 March 2019; Accepted: 9 April 2019; Published: 27 April 2019



Abstract: This paper presents an experimental study on the AC breakdown voltages of Refined, Bleached and Deodorized Palm Oil (RBDPO) Olein and Coconut Oil (CO) in the presence of conductive (Iron (II,III) Oxide, Fe₃O₄), semi-conductive (Copper (II) Oxide, CuO) and insulative (Aluminium Oxide, Al₂O₃) nanoparticles without and with surfactant. The type of surfactant used in this study was Cetyl Trimethyl Ammonium Bromide (CTAB). The volume concentrations range of Fe₃O₄, CuO and Al₂O₃ was varied from 0.001% to 0.05%. Transmission Electron Microscope (TEM) was used to characterize the nanoparticles in RBDPO and CO. AC breakdown voltage tests were carried out for RBDPO and CO of which the AC breakdown voltage at 1% probability was determined based on Weibull distribution. It is found that only Al₂O₃ can improve the average AC breakdown voltage of RBDPO and CO. The AC breakdown voltages at 1% probability for RBDPO and CO can be improved through introduction of Fe₃O₄, CuO and Al₂O₃ at certain volume concentrations. Al₂O₃ provides the highest enhancement of AC breakdown voltages at 1% probability for RBDPO and CO with the highest percentage of improvement can be up to 52%. CTAB has no clear effect on the improvement of AC breakdown voltages of RBDPO and CO based Fe₃O₄, CuO and Al₂O₃ nanofluids.

Keywords: AC breakdown voltage; refined bleached and deodorized palm oil; coconut oil; Fe₃O₄; CuO; Al₂O₃; nanofluids

1. Introduction

It is known that nanoparticles are able to enhance the cooling properties, thermal conductivity/diffusivity and electrical characteristics of insulation fluids [1–4]. Previous works have examined thoroughly the electrical parameters of nanofluids which include the initiation voltage, discharge propagation and streamers [5,6]. The effects of nanoparticles on insulation fluids are known to be dependent upon the intrinsic properties, volume concentrations, solid-liquid contact areas, suspension by surfactants and synthesis methods [7,8].

The synthesis method of dispersing nanoparticles in insulation fluids can be carried out either by one- or two-step methods. In one-step method, the dispersion of nanoparticles is carried out directly

into the base fluids. However, this method is not recommended for large quantities of nanofluids due to the incomplete reaction and stabilization [9,10]. In two-step method, nanoparticles are dispersed into the base fluids by automated mixers such as magnetic stirrer, high-shear mixers and bead mills. Sonication is used to ensure uniform dispersion of nanofluids and surfactant decrease agglomeration and prevent sedimentation of nanofluids. In addition, the electrostatic and steric stabilities of insulation fluids against agglomeration can be improved with introduction of surfactants. Surfactants could adsorb at the interface between nanoparticle and insulating fluid and change the dielectric and thermal characteristics of nanofluids [8,11].

Previous works have examined the mineral oil and vegetable oil based nanofluids based on electrically conductive, semi-conductive and insulative nanoparticles which focus on the AC/lightning breakdown voltage, streamer, partial discharge, dielectric properties and thermal ageing [3–6,10–21]. Majority of the studies focus on the AC breakdown voltages examination whereby different types of nanoparticles such as Iron (II,III) Oxide (Fe_3O_4), Iron (III) Oxide (Fe_2O_3), Zinc Oxide (ZnO), Silicon Oxide (SiO_2), Titanium Oxide (TiO_2), Aluminium Oxide (Al_2O_3), Copper (II) Oxide (CuO), Zirconium Dioxide (ZrO_2), Multi-wall Carbon Nanotubes (MWCNT) and Aluminium Nitride (AlN) have been considered [4,5,11,19–38]. Both mineral- and vegetable-based nanofluids have been tested for AC breakdown voltage and the performance improvements up to 256% and 63% have been recorded [35,37]. In addition, different types of surfactants such as Cetyl Trimethyl Ammonium Bromide (CTAB), oleic acid, Sodium Dodecyl Sulfonate (SDS), silane coupling agent Z6011, Sodium Dodecyl Benzene Sulfonate (SDBS) and Octadecylamine Acetate (ODA) have been examined of which several noticeable impacts are observed [5,11,22,25–27,30,33,36,38]. Overall, the AC breakdown voltage studies of nanofluids conclude that the positive effects will normally take place at low level of volume percentage concentrations of nanoparticles [11,22,27,30]. In addition, the types of surfactants used for the nanofluids can also affect the AC breakdown voltage performances [27,38].

Most of the AC breakdown voltage studies on vegetable-based nanofluids focused on crops such as rapeseed, palm, soybean, corn and coconut [5,20,22,24–26,29,33,35]. A study in Reference [5] reveals that the average AC breakdown voltage of rapeseed oil increases by 20% with the introduction of Fe_3O_4 and oleic acid [5]. Other study shows that the introduction of Fe_3O_4 could reduce the AC breakdown voltage at 1% probability for Palm Fatty Acid Ester (PFAE) by 5%. However, both TiO_2 and Al_2O_3 could increase the AC breakdown voltage at 1% probability for PFAE by 14% and 7% respectively [20]. In the presence of ZnO and TiO_2 , the AC breakdown voltages of soybean ester oil can increase by 41% and 63% while palm ester oil can increase by 44% and 54% respectively [25]. Other studies in References [24,29] show that the introduction of TiO_2 and SiO_2 in natural ester FR3, increase the AC breakdown voltage by 31% and 33%. Currently, the studies on the effect of nanoparticles on Refined, Bleached and Deodorized Palm Oil (RBDPO) Olein and Coconut Oil (CO) are still limited. In addition, further knowledge is needed to confirm the impact of Fe_3O_4 , CuO and Al_2O_3 on the AC breakdown voltage performances on vegetable oils. This paper presents the initiative to further understand the impact of three types of nanoparticles on the AC breakdown voltage performances of RBDPO and CO. Conductive (Fe_3O_4), semi-conductive (CuO) and insulative (Al_2O_3) nanoparticles are used in this study. The impact of CTAB is also examined and all samples are tested for AC breakdown voltages. Weibull distribution is used for the analysis on the AC breakdown voltage at 1% probability.

2. Materials and Methods

2.1. Materials

Two types of RBDPO Olein were examined as samples for palm oil. Meanwhile, virgin CO was used for the other type of vegetable oil. The fats content and vitamin E and A of the RBDPO and CO are shown in Table 1. The distribution of the fatty acids for all RBDPO and CO were determined by Gas Chromatography (GC) based on MPOB test methods, p.3.4:2004 and p.3.5:2004 [39]. The contents

of saturated fats and unsaturated fats among the RBDPO are almost similar and it is lower than CO which is dominated by saturated fats, as shown in Table 1.

Table 1. Fatty acid content, fat and vitamin E/A content of all samples.

Types of Fats	Types of Fatty Acids	RBDPOA		RBDPOB		CO	
		GC (%)	MD (g)	GC (%)	MD (g)	GC (%)	MD (g)
Saturated	C6: Caproic	-	-	-	-	-	-
	C8: Caprylic	-	-	-	-	-	-
	C10: Capric	-	-	-	-	-	-
	C12: Lauric	0.3	45.4	0.3	43.0	48.6	92.8
	C14: Myristic	1.1	-	0.9	-	20.0	-
	C16: Palmitic	37.7	-	39.3	-	9.5	-
	C18: Stearic	3.9	-	4.2	-	3.2	-
Monounsaturated	C18: Oleic	42.3	43.0	43.0	43.0	6.0	3.6
Polyunsaturated	C18: Linoleic	12.4	11.6	10.4	14.0	1.1	3.6
	C18: Linolenic	0.3	-	0.2	-	-	-
Vitamin E		-	4.4×10^{-3}	-	75×10^{-3}	-	-
Vitamin A		-	264×10^{-6}	-	-	-	-

* GC = Gas Chromatography; MD = Manufacturer's Datasheet; RBDPOA = Refined, Bleached and Deodorized Palm Oil A; RBDPOB = Refined, Bleached and Deodorized Palm Oil B; CO = Coconut Oil.

The types of nanoparticles used in this study were conductive nanoparticle, Fe_3O_4 , semi-conductive nanoparticle, CuO and insulative nanoparticle, Al_2O_3 . The basic properties of Fe_3O_4 , CuO and Al_2O_3 nanoparticles are shown in Table 2. The Al_2O_3 size is lower than both Fe_3O_4 and CuO. The colour of Fe_3O_4 and CuO are black while Al_2O_3 is white. The densities of Fe_3O_4 , CuO and Al_2O_3 are 5.17 g/cm^3 , 6.31 g/cm^3 and 3.96 g/cm^3 respectively.

Table 2. Basic properties of Fe_3O_4 , CuO and Al_2O_3 nanoparticles [6,40].

Properties	Fe_3O_4	CuO	Al_2O_3
Size (nm)	50–100	<50	40
Appearance colour	Black	Black	White
Density (g/cm^3)	5.17	6.31	3.96
Relative permittivity	80	18.1	9.9
Electrical conductivity (S/m)	1×10^4 – 1×10^5	1×10^7	1×10^{-12}
Thermal conductivity (W/m.K)	4–8	76.5	30

To attain suspension stability against sedimentation of nanoparticles, CTAB was used in this study. The shape of CTAB is solid spherical and white in colour as shown in Table 3.

Table 3. Basic properties of Cetyl Trimethyl Ammonium Bromide (CTAB) nanoparticles [6,40].

Properties	CTAB
Description	Cationic
Form	Solid
Colour	White
Melting point ($^\circ\text{C}$)	248–251
Flash point ($^\circ\text{C}$)	244
Flammability	Not flammable

2.2. Preparation of Nanofluids

Three times filtration of all RBDPO and CO were carried by a membrane filter with a pore size of $0.2 \mu\text{m}$ before the synthesis process. The first part of synthesis procedure of RBDPO and CO based Fe_3O_4 , CuO and Al_2O_3 nanofluids was carried out without CTAB as shown in Figure 1. The Fe_3O_4 , CuO and Al_2O_3 were first dispersed individually into either RBDPO and CO through a Fisher Scientific

isotemp heated magnetic stirrer at 800 rpm. After 30 min of stirring, the oil samples were rested at ambient temperature for 30 min. Next, the oil samples were dried through an air circulating oven at 85 °C for 48 h.

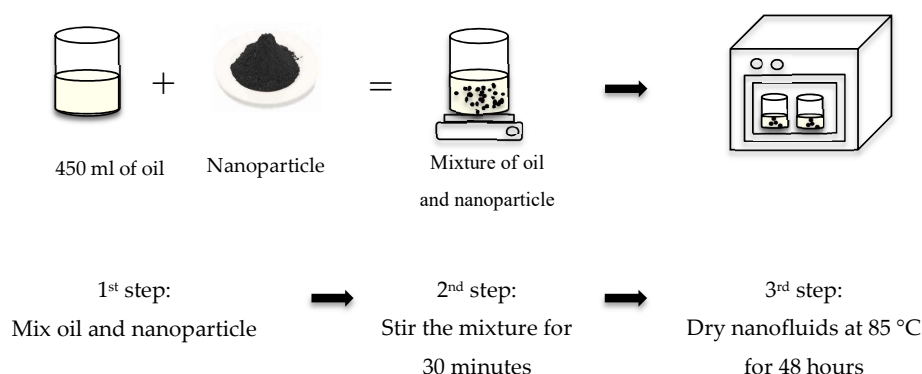


Figure 1. The synthesis process of oil and nanoparticles without Cetyl Trimethyl Ammonium Bromide (CTAB).

For the second part of synthesis with CTAB, RBDPO and CO were suspended individually with CTAB for 30 min by a magnetic stirrer as shown in Figure 2. The concentration of CTAB under study is 50% of the volume concentration of nanoparticles. It is based on the similar study in Reference [33] where the optimum concentration of surfactants is found at that concentration level. Next, the Fe_3O_4 , CuO and Al_2O_3 were added individually into oil samples of which the stirring time was maintain for 30 min. Ultrasonic Homogenizer—Model 300VT was used to ensure well dispersion of Fe_3O_4 , CuO, Al_2O_3 and CTAB in the oil samples and to reduce the agglomeration time. The sonication was carried out for 1 h. In total, 30 min of resting time at ambient temperature was given to the oil samples before it was subjected to drying process in an air circulating oven for 48 h at 85 °C. The final procedure was to rest the oil samples for 24 h at ambient temperature before the AC breakdown voltage measurement. The oil samples were stirred by magnetic stirrer during the AC breakdown voltage test as per ASTM D1816 [41]. The volume percentage concentrations of Fe_3O_4 , CuO and Al_2O_3 used in this study were 0.001%, 0.025%, 0.035% and 0.05%. The moisture for the nanofluids could not be determined after the drying procedure for both synthesis processes due to difficulties to assess the commercial moisture measurement tester. However, based on the same drying procedure for base oil, the moisture ranges for RBDPOA, RBDPOB and CO are 143 ppm, 134 ppm and 150 ppm based on measurements by Metrohm 831 Karl Fischer (KF) Coulometer as per ASTM D6304 [42].

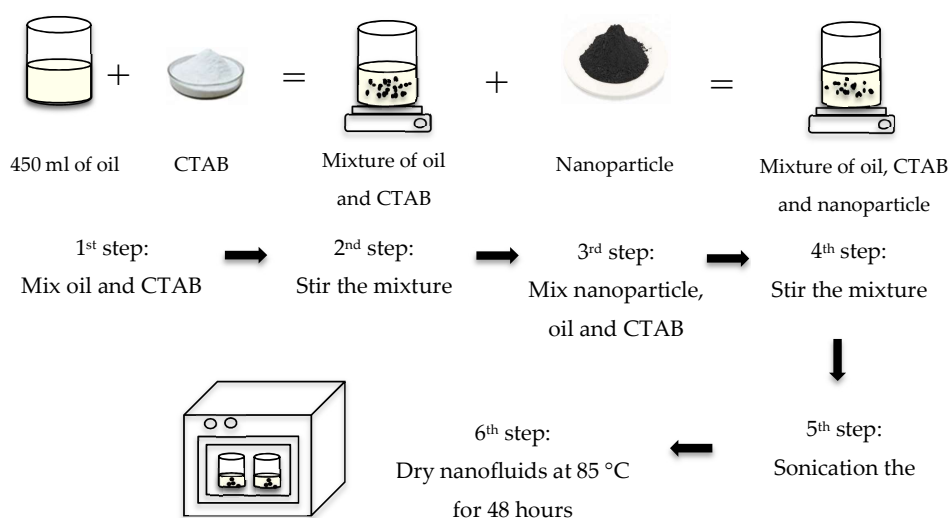


Figure 2. The synthesis process of oil and nanoparticles with CTAB.

2.3. Nanoparticle Characterization

The morphology of the RBDPO and CO based Fe_3O_4 , CuO and Al_2O_3 nanofluids were observed by JEOL JEM-2100F high-resolution transmission electron microscope (HRTEM). The point and lattice resolutions of the equipment can be up to 0.23 nm and 0.1 nm. The oil samples were first diluted with distilled water and one drop of diluted sample was placed on the copper grid. Next, the copper grid was placed for 15 min on a drop of uranyl acetate solution for staining purpose before placed in filter paper. Overnight drying of the copper grid was carried out at room temperature before viewed by HRTEM. For this measurement, only RBDPO and CO based Fe_3O_4 , CuO and Al_2O_3 nanofluids with volume percentage concentrations of 0.05% were analyzed.

2.4. AC Breakdown Voltage

The AC breakdown voltage test was carried out based on ASTM D1816 at ambient temperature ranging between 25 °C and 34 °C. The AC breakdown voltage was carried by BAUR DPA 75C of which the oil samples were poured into a 500 mL test cell [41]. The equipment can measure AC breakdown voltage up to 75 kV \pm 1 kV. VDE electrodes, each with a diameter of 36 mm were used for the test. The gap distance between electrodes was set to 1 mm. A uniform rise rate of 0.5 kV/s was subjected to the oil samples until the breakdown. The oil samples were stirred continuously during the breakdown. For each of the oil samples, 5 min resting interval time was given to ensure the breakdown by-products and bubbles dispersed out from the electrodes. In total, the average of 50 breakdown measurements was recorded for analysis.

3. Results

3.1. Effect of Fe_3O_4 Nanoparticle on RBDPO and CO

Transmission Electron Microscope (TEM) images of the RBDPOA, RBDPOB and CO after 0.05 % addition of Fe_3O_4 without and with CTAB can be seen in Figure 3. The agglomerations of Fe_3O_4 for oil samples without CTAB shown in Figure 3a–c are more apparent as compared to oil samples with CTAB shown in Figure 3d,e.

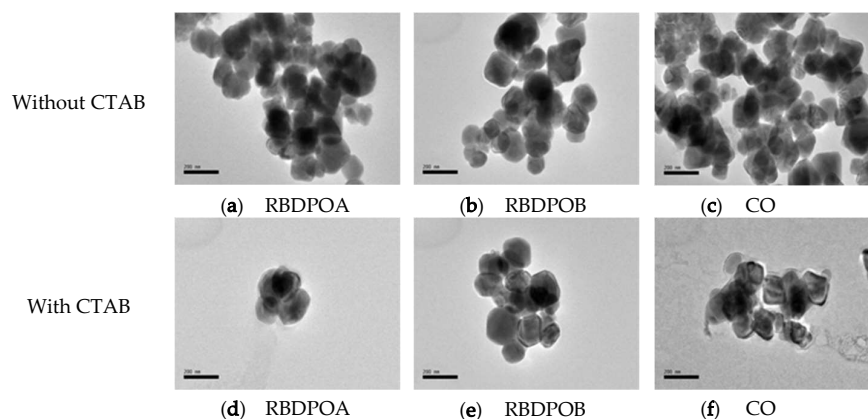


Figure 3. Transmission Electron Microscope (TEM) images for (a) Refined, Bleached and Deodorized Palm Oil A (RBDPOA), (b) Refined, Bleached and Deodorized Palm Oil B (RBDPOB) and (c) Coconut Oil (CO) without the presence of CTAB and (d) RBDPOA, (e) RBDPOB and (f) CO with the presence of CTAB at 0.05% of Fe_3O_4 .

Generally, the introduction of Fe_3O_4 generally causes reduction of AC breakdown voltage for RBDPO and CO without and with CTAB. Without CTAB, the AC breakdown voltage reduction trend for RBDPOA is almost linear as the volume concentrations of Fe_3O_4 increases from 0.001% to 0.05% as shown in Figure 4a. The AC breakdown voltage of RBDPOA decreases by 33% after addition 0.05%

of Fe_3O_4 . The same pattern is observed for RBDPOB except that there is a minor increment of AC breakdown voltage after 0.05% addition of Fe_3O_4 . The AC breakdown voltage trend for CO is different from RBDPO where 0.001% of Fe_3O_4 initially causes significant reduction of AC breakdown voltage. With 0.025% addition of Fe_3O_4 , the AC breakdown voltage of CO increases almost exponentially as the volume concentration of Fe_3O_4 increase to 0.05%.

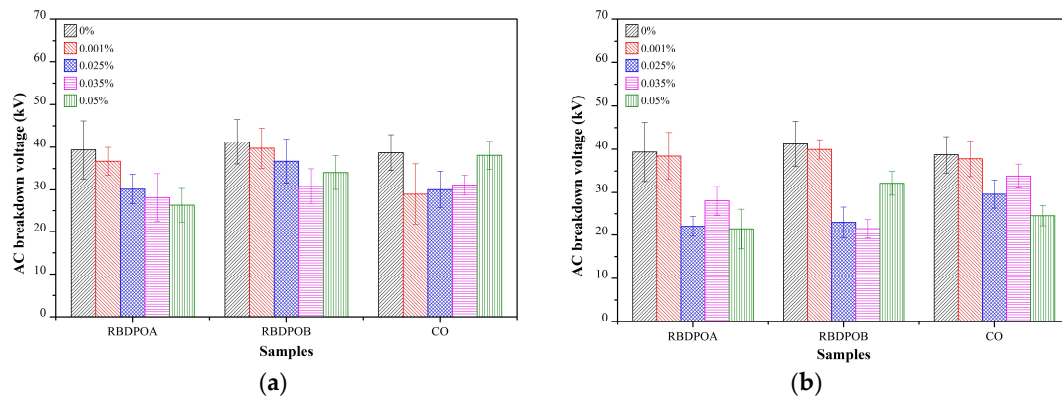


Figure 4. Effect of Fe_3O_4 on the AC breakdown voltage of RBDPO and CO (a) without CTAB and (b) with CTAB.

The reductions of AC breakdown voltages are higher for oil samples with CTAB than without CTAB as shown in Figure 4b. Significant reductions of AC breakdown voltages are found for the oil samples after 0.025% addition of Fe_3O_4 . The highest percentages of AC breakdown voltage reductions for RBDPOA, RBDPOB and CO are 46%, 48%, 37% after 0.05%, 0.035%, 0.05% addition of Fe_3O_4 respectively.

The AC breakdown voltages of different concentration of Fe_3O_4 at 1% probability are tabulated in Table 4 which have been determined by cumulative Weibull distribution function with scale parameter (α), shape parameter (β) and measured data (t) shown in Equation (1).

$$F(t|\alpha,\beta) = 1 - e^{-(t/\alpha)^\beta} \quad (1)$$

Table 4. AC breakdown voltage of Refined, Bleached and Deodorized Palm Oil (RBDPO) and Coconut Oil (CO) at 1% probability at different concentration of Fe_3O_4 .

Samples	Volume of Concentration (%)	Breakdown Voltage at 1% Probability (kV)	
		Without CTAB	With CTAB
RBDPOA	0	21.60	21.60
	0.001	27.69	25.27
	0.025	20.72	14.90
	0.035	14.82	17.88
	0.05	15.86	10.40
RBDPOB	0	25.88	25.88
	0.001	27.17	33.93
	0.025	24.58	13.81
	0.035	19.68	15.29
	0.05	24.32	25.88
CO	0	27.21	27.21
	0.001	11.64	27.32
	0.025	18.96	19.54
	0.035	24.31	26.44
	0.05	30.03	17.29

It is shown that 0.001% addition of Fe_3O_4 can increase the AC breakdown voltages at 1% probability for most of the oil samples without and with CTAB as shown in Table 4. Only CO without CTAB shows enhancement of AC breakdown voltages at 1% probability at volume concentration of 0.05%. The highest percentage of improvement for AC breakdown voltage at 1% probability can be up to 31% for RBDPOB with CTAB. There is no clear improvement effect of CTAB on the of AC breakdown voltage at 1% probability for Fe_3O_4 .

3.2. Effect of CuO Nanoparticle on RBDPO and CO

The TEM images for CuO disperse in RBDPO and CO without and with CTAB at volume concentration of 0.05% can be seen in Figure 5. For both RBDPO, the agglomerations of CuO decrease as CTAB is added as shown in Figure 5a,b,d,e. On the other hand, the TEM images in Figure 5c,f show no clear effect of CTAB on the agglomerations of CuO in CO.

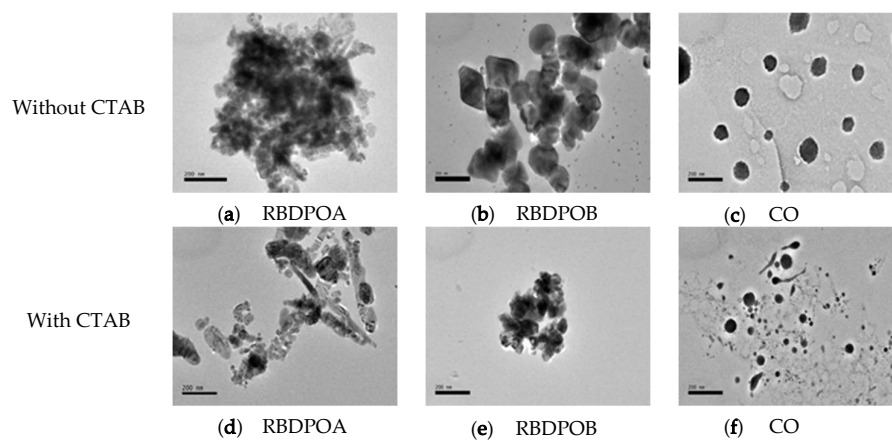


Figure 5. TEM images for (a) RBDPOA, (b) RBDPOB and (c) CO without the presence of CTAB and (d) RBDPOA, (e) RBDPOB and (f) CO with the presence of CTAB at 0.05% of CuO.

A similar pattern is observed as Fe_3O_4 for CuO whereby majority of the AC breakdown voltages for RBDPO and CO decrease as the volume concentration of CuO increases. Without CTAB, the AC breakdown voltage of RBDPOA initially decreases as the volume concentration of CuO increases to 0.025% as shown in Figure 6a. As the volume concentration of CuO increases to 0.05%, the AC breakdown voltage of RBDPOA slightly increases but at a much lower level than the base oil. RBDPOB experiences significant reduction of AC breakdown voltage with 0.001% addition of CuO. As the volume concentration of CuO increases from 0.025% to 0.05%, the AC breakdown voltage of RBDPOB increases almost linearly to a final value of 34.1 kV. The AC breakdown voltage of CO decreases almost exponentially as the volume concentration of CuO increases.

The introduction of CTAB leads to further reduction of AC breakdown voltages for the oil samples as shown in Figure 6b. The oil samples show a steady decrement trend of AC breakdown voltages as the volume concentrations of CuO increases. The final AC breakdown voltages of RBDPOA, RBDPOB and CO after 0.05% addition of CuO are 16.3 kV, 16.8 kV and 16.1 kV respectively.

The introduction of CuO can only improve AC breakdown voltages at 1% probability for RBDPOA as seen Table 5. The highest percentages of AC breakdown voltage improvements for without and with CTAB are 16% and 27% after 0.035% and 0.001% addition of CuO. After introduction of CuO, RBDPOB and CO experience significant reductions of AC breakdown voltages at 1% probability either without or with CTAB.

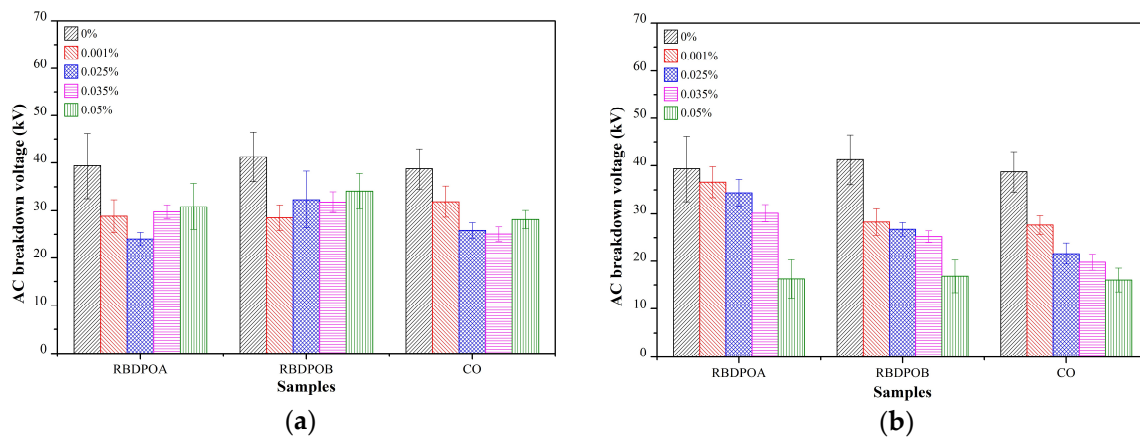


Figure 6. Effect of CuO on AC breakdown voltage of RBDPO and CO (a) without CTAB and (b) with CTAB.

Table 5. AC breakdown voltage of RBDPO and CO at 1% probability at different concentration of CuO.

Samples	Volume of Concentration (%)	Breakdown Voltage at 1% Probability (kV)	
		Without CTAB	With CTAB
RBDPOA	0	21.60	21.60
	0.001	19.36	27.44
	0.025	17.84	26.13
	0.035	25.01	24.23
	0.05	18.42	6.36
RBDPOB	0	25.88	25.88
	0.001	20.02	21.56
	0.025	16.76	22.22
	0.035	24.39	21.50
	0.05	22.60	7.98
CO	0	27.21	27.21
	0.001	22.35	21.21
	0.025	21.02	15.41
	0.035	19.65	15.01
	0.05	22.67	9.33

3.3. Effect of Al₂O₃ Nanoparticle on RBDPO and CO

The effect of CTAB on the agglomerations of Al₂O₃ in the oil samples is not as clear as Fe₃O₄ and CuO as shown in Figure 7. For RBDPOA, it seems that the introduction of CTAB increases the agglomerations of Al₂O₃ as seen in Figure 7d. The agglomeration for RBDPOB seems almost unchanged with introduction of CTAB as shown in Figure 7e. On the other hand, CTAB reduces the agglomerations of Al₂O₃ for CO as seen in Figure 7f.

Without CTAB, there are increment patterns of AC breakdown voltages for RBDPOA and CO as the volume concentration of Al₂O₃ increases as seen in Figure 8a. The AC breakdown voltage of RBDPOA increases by 12% with 0.035% addition of Al₂O₃. Meanwhile, 0.05% addition of Al₂O₃ increases the AC breakdown voltage of CO by 12%. For RBDPOB, the AC breakdown voltage fluctuates at 40.6 kV and 42.1 kV as the volume concentration of Al₂O₃ increases. Only a minor increment of AC breakdown voltage for RBDPOB is found.

The patterns of AC breakdown voltages are slightly different for oil samples with CTAB as compare to without CTAB as seen in Figure 8b. The AC breakdown voltage of RBDPOA still shows AC breakdown voltage increment pattern as the volume concentration of Al₂O₃ increases. The highest percentage of AC breakdown voltage increment for RBDPOA is 18% after 0.035% addition of Al₂O₃.

For RBDPOB, the AC breakdown voltage slightly decreases as 0.001% of Al_2O_3 is added and maintains as the volume concentration of Al_2O_3 increases. The AC breakdown voltage of CO decreases steadily as the volume concentration of Al_2O_3 increases until 0.035%. The AC breakdown voltage increases by 7% with 0.05% addition of Al_2O_3 .

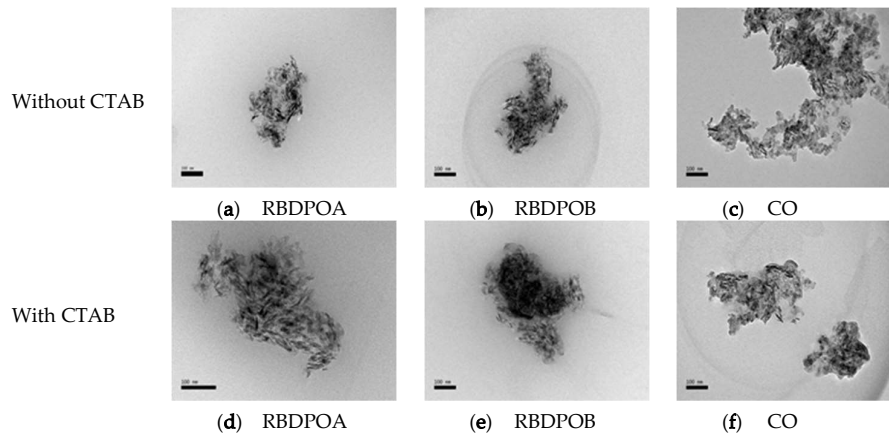


Figure 7. TEM images for (a) RBDPOA, (b) RBDPOB and (c) CO without the presence of CTAB and (d) RBDPOA, (e) RBDPOB and (f) CO with the presence of CTAB at 0.05% of Al_2O_3 .

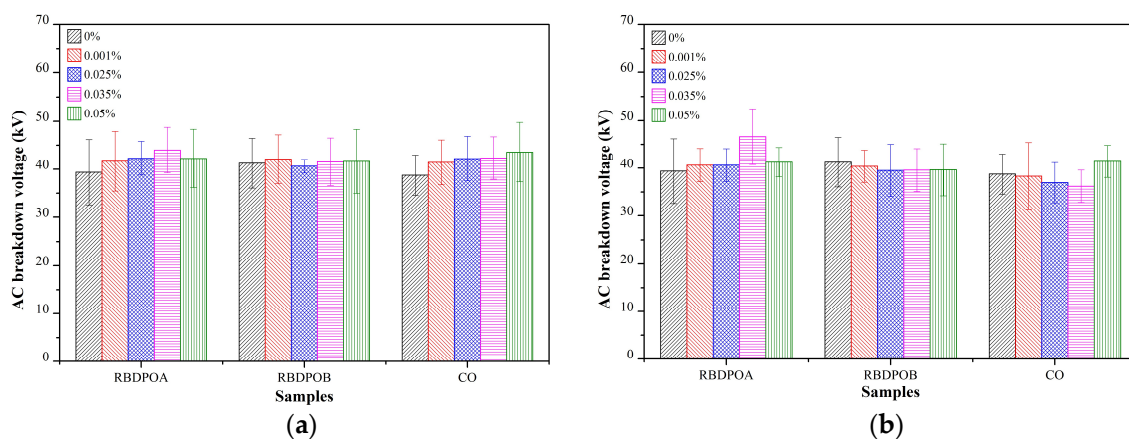


Figure 8. Effect of Al_2O_3 on AC breakdown voltage of RBDPO and CO (a) without CTAB and (b) with CTAB.

Apparent improvements of AC breakdown voltages at 1% probability are observed with introduction of Al_2O_3 either without or with CTAB as shown in Table 6. Without CTAB, the AC breakdown voltage at 1% probability for RBDPOA and RBDPOB can increase up to 40% and 33% with 0.025% addition Al_2O_3 . The highest AC breakdown voltage improvement at 1% probability for CO can be up to 7%. The introduction of CTAB further improves the AC breakdown voltage at 1% probability for RBDPOA of which the highest percentage of increment can be up to 52% with 0.05% addition of Al_2O_3 . The same pattern is observed for CO whereby, the AC breakdown voltage at 1% probability increases by 15% with 0.05% addition of Al_2O_3 . However, the same significant improvement effect is not found for RBDPOB where the presence of CTAB can only increase the AC breakdown voltage at 1% probability up to 15% only with 0.001% addition of Al_2O_3 .

Table 6. AC breakdown voltage of RBDPO and CO at 1% probability at different concentration Al₂O₃.

Samples	Volume of Concentration (%)	Breakdown Voltage at 1% Probability (kV)	
		Without CTAB	With CTAB
RBDPOA	0	21.60	21.60
	0.001	23.57	30.75
	0.025	30.32	31.68
	0.035	28.50	32.24
	0.05	23.49	32.81
RBDPOB	0	25.88	25.88
	0.001	28.70	29.65
	0.025	34.35	25.03
	0.035	27.85	26.92
	0.05	23.47	25.99
CO	0	27.21	27.21
	0.001	28.10	20.98
	0.025	28.54	24.45
	0.035	29.12	24.05
	0.05	27.44	31.20

4. Discussion

Based on the study, only insulative nanoparticle, Al₂O₃ could slightly improve the average AC breakdown voltage of RBDPO and CO either without or with CTAB as shown in Figure 8. In addition, the improvement of AC breakdown voltages of the oil samples take place at no specific volume concentrations of Al₂O₃ similar as reported in Reference [43]. It is due to the agglomerations of nanoparticles in oil samples could not be controlled with the increment of volume concentration of nanoparticles which in turn lead to the difficulties to identify the optimum concentration for AC breakdown voltage improvement [8,17]. Previous study has shown that Fe₃O₄ could improve the average AC breakdown voltage of vegetable oil such as rapeseed oil, natural ester FR3 and PFAE [5,20,44]. However, the current study shows that Fe₃O₄ could not improve the average AC breakdown voltages of RBDPO and CO either without or with CTAB as shown in Figure 4. It is possibly due to differences on the chemical composition between RBDPO/CO and other types of vegetable oils. Further investigation on this aspect is needed to confirm the findings in the future. CuO has shown to be capable of improving the average AC breakdown voltage of mineral oil [45]. The current study shows that there are no improvements on the average AC breakdown voltages of RBDPO and CO either without or with CTAB as shown in Figure 6. At the moment, there is yet any study on the effect of CuO on the average AC breakdown voltage for other types of vegetable oils. Further investigation is needed to extract the knowledge of the negative effect of CuO on the average AC breakdown voltage of RBDPO and CO through extensive study at the molecular level.

Meanwhile, the effects of CTAB on the AC breakdown voltages of RBDPO and CO filled with nanoparticles under study are not clear. Previous studies have shown that CTAB is one of the most common surfactants that can be used to reduce the agglomeration and improve dispersion of the nanoparticles in mineral oil, palm oil, coconut oil and soybean ester oil [11,25,26]. Previous studies on the palm ester oil and soybean ester oil based ZnO and TiO₂ nanofluids show increments of AC breakdown voltages with introduction of CTAB. This is due to the fact that a charge trapping capability increases as a result of improvement of the nanoparticles aggregation [25,33]. However, the improvement of AC breakdown voltage of RBDPO based CuO nanofluid in the presence of CTAB found in Reference [33] is somehow contradictory to the current study. The repeated test in the current study reveals that the AC breakdown voltages of the oil samples further decreases as CTAB is introduced. The finding in the current study as shown in Figures 4b and 6b is in line with Reference [26], which shows that CTAB has no clear impact on the AC breakdown voltage of RBDPO based TiO₂ nanofluids. This is possibly due to limited compatibility of CTAB with certain nanoparticles

and its viscosity effect. Previous study on mineral based TiO₂ nanofluids reveals that the attraction force between the nanoparticles and CTAB can also lead to the agglomerations among these opposite charged particles [11]. These agglomerations could initiate low charge trapping and deformation in the electric field which to a certain extent affect the AC breakdown voltage [8,11]. The high viscosities of RBDPO and CO could also cause suspension of nanoparticles which in turn lead to no apparent positive impact of CTAB on AC breakdown voltages.

Generally, the current findings show that the introduction of nanoparticles at certain volume concentrations could increase the AC breakdown voltage at 1% probability for RBDPO and CO either with or without CTAB as shown in Tables 4–6. All nanoparticles show positive impact on the AC breakdown voltage at 1% probability of RBDPO and CO at certain volume concentrations of which Al₂O₃ gives the highest improvement. From the practical point of view, the improvement of the AC breakdown voltage at the lowest probability could help to improve the design of transformers filled with vegetable-based nanofluids in the future.

5. Conclusions

The AC breakdown voltages of RBDPOA, RBDPOB and CO slightly increase with the introduction of Al₂O₃ either without or with CTAB. RBDPO and CO show clear decrement trends of average AC breakdown voltages with the introduction of Fe₃O₄ and CuO either without and with CTAB. Significant improvement of AC breakdown voltage at 1% probability is found with the introduction of Fe₃O₄, CuO and Al₂O₃ at certain volume concentrations. However, there is no clear knowledge that can be obtained on the best volume concentration of nanoparticles which can give the optimum improvement of AC breakdown voltages of RBDPO and CO. The introduction of CTAB gives improvement on the agglomeration and increases the dispersion of the nanoparticles in majority of the RBDPO and CO based on TEM imaging. However, this phenomenon has no direct effect on the AC breakdown voltages of RBDPO and CO, which implies the complexity of vegetable-based nanofluids fundamentals application in transformers.

Author Contributions: The research study was successfully completed with contributions from all authors. The main research idea, experimental works, and manuscript preparation were contributed by N.A.M. N.A. contributed to the manuscript preparation and research idea. J.J., M.Z.A.A.K. and R.Y. assisted with finalizing the research work and manuscript. Z.Y. provided several suggestions from an industrial perspective. All authors revised and approved the publication of the paper.

Acknowledgments: The authors would like to thank Ministry of Education and Universiti Putra Malaysia for the funding under PUTRA IPS and IPB schemes (GP-IPS/2015/9462100), (GP-IPB/2014/9440801). Special thanks to Hyrax Oil Sdn. Bhd and Malaysia Transformer Manufacturing Sdn. Bhd. for the technical support.

Conflicts of Interest: The authors declare no conflicts of interest.

Nomenclature

α	Scale parameters
β	Shape parameters
t	Measured data
kV	Kilo Voltage
Fe ₃ O ₄	Iron (II,III) Oxide
Fe ₂ O ₃	Iron (III) Oxide
ZnO	Zinc Oxide
SiO ₂	Silicone Oxide
TiO ₂	Titanium Oxide
Al ₂ O ₃	Aluminium Oxide
CuO	Copper (II) Oxide
ZrO ₂	Zirconium Dioxide
MWCNT	Multi-wall Carbon Nanotubes
AlN	Aluminium Nitride

References

1. Khaled, U.; Beroual, A. AC Dielectric Strength of Mineral Oil-Based Fe₃O₄ and Al₂O₃ Nanofluids. *Energies* **2018**, *11*, 3505. [[CrossRef](#)]
2. Raymon, A.; Sakthibalan, S.; Cinthal, C.; Subramaniraja, R.; Yuvaraj, M. Enhancement and Comparison of Nano-ester Insulating Fluids. *IEEE Trans. Dielectr. Electr. Insul.* **2016**, *23*, 892–900. [[CrossRef](#)]
3. Du, B.; Li, J.; Wang, F.; Yao, W.; Yao, S. Influence of Monodisperse Fe₃O₄ Nanoparticle Size on Electrical Properties of Vegetable Oil-based Nanofluids. *J. Nanomater.* **2015**, *2015*, 560352. [[CrossRef](#)]
4. Lv, Y.Z.; Wang, J.; Yi, K.; Wang, W.; Li, C. Effect of Oleic Acid Surface Modification on Dispersion Stability and Breakdown Strength of Vegetable Oil-based Fe₃O₄ Nanofluids. *Integr. Ferroelectr.* **2015**, *163*, 21–28. [[CrossRef](#)]
5. Li, J.; Zhang, Z.; Zou, P.; Grzybowski, S.; Zahn, M. Preparation of a Vegetable Oil-based Nanofluid and Investigation of Its Breakdown and Dielectric Properties. *IEEE Electr. Insul. Mag.* **2012**, *28*, 43–50. [[CrossRef](#)]
6. Hwang, J.G.; Zahn, M.; O'Sullivan, F.M.; Petterson, L.A.A.; Hjortstam, O.; Liu, R. Effect of Nanoparticle Charging on Streamer Development in Transformer Oil-based Nanofluids. *J. Appl. Phys.* **2010**, *107*, 1–17. [[CrossRef](#)]
7. Xuan, Y.; Li, Q. Heat Transfer Enhancement of Nanofluids. *Int. J. Heat Fluid Flow* **2000**, *21*, 58–64. [[CrossRef](#)]
8. Rafiq, M.; Lv, Y.Z.; Li, C. A Review on Properties, Opportunities, and Challenges of Transformer Oil-based Nanofluids. *J. Nanomater.* **2016**, *2016*, 8371560. [[CrossRef](#)]
9. Yu, W.; Xie, H.Q. A Review on Nanofluids: Preparation, Stability Mechanism and Applications. *J. Nanomater.* **2012**, *2012*, 435873. [[CrossRef](#)]
10. Lv, Y.Z.; Zhou, Y.; Li, C.R.; Wang, Q.; Qi, B. Recent Progress in Nanofluids Based on Transformer Oil: Preparation and Electrical Insulation Properties. *IEEE Electr. Insul. Mag.* **2014**, *30*, 23–32. [[CrossRef](#)]
11. Atiya, E.G.; Mansour, D.E.A.; Khattab, R.M.; Azmy, A.M. Dispersion Behavior and Breakdown Strength of Transformer Oil Filled with TiO₂ Nanoparticles. *IEEE Trans. Dielectr. Electr. Insul.* **2015**, *22*, 2463–2472. [[CrossRef](#)]
12. Ranjan, N.; Pratash, R.T.A.R.; Roy, N.K. Ageing Performance on Mineral Oil using ZnO Nanofluids. *Int. J. Innov. Eng. Technol.* **2016**, *6*, 155–162.
13. Li, J.; Du, B.; Wang, F.; Yao, W.; Yao, S. The Effect of Nanoparticle Surfactant Polarization on Trapping Depth of Vegetable Insulating Oil-based Nanofluids. *Phys. Lett. A* **2016**, *380*, 604–608. [[CrossRef](#)]
14. Lv, Y.Z.; Du, Y.F.; Zhou, J.Q.; Li, X.X.; Chen, M.T.; Li, C.R.; Wang, G.L. Nanoparticle Effect on Electrical Properties of Aged Mineral Oil based Nanofluids. *CIGRE* **2012**, *D1-106*, 1–6.
15. Chen, Y.; Wu, J. Investigation on Relationship between Breakdown Strength Enhancement of Composites and Dielectric Characteristics of Nanoparticle. *IEEE Trans. Dielectr. Electr. Insul.* **2016**, *23*, 927–934. [[CrossRef](#)]
16. Ghasemi, J.; Jafarmadar, S.; Nazari, M. Effect of Magnetic Nanoparticles on the Lightning Impulse Breakdown Voltage of Transformer Oil. *J. Magn. Mater.* **2015**, *389*, 148–152. [[CrossRef](#)]
17. Du, Y.F.; Lv, Y.Z.; Zhou, J.Q.; Li, X.X.; Li, C.R. Breakdown Properties of Transformer Oil-based TiO₂ Nanofluid. In Proceedings of the Annual Report Conference on Electrical Insulation and Dielectric Phenomena (CEIDP'10), West Lafayette, IN, USA, 17–20 October 2010; pp. 1–4.
18. Lee, J.C.; Seo, H.S.; Kim, Y.J. The Increased Dielectric Breakdown Voltage of Transformer Oil-based Nanofluids by an External Magnetic Field. *Int. J. Therm. Sci.* **2012**, *62*, 29–33. [[CrossRef](#)]
19. Du, Y.F.; Lv, Y.Z.; Li, C.R.; Chen, M.; Zhong, Y.X.; Zhou, J.Q.; Li, X.X.; Zhou, Y. Effect of Semiconductive Nanoparticles on Insulating Performances of Transformer Oil. *IEEE Trans. Dielectr. Electr. Insul.* **2012**, *19*, 770–776.
20. Mohamad, M.S.; Zainuddin, H.; Ab Ghani, S.; Chairul, I.S. AC Breakdown Voltage and Viscosity of Palm Fatty Acid Ester (PFAE) Oil-Based Nanofluids. *J. Electr. Eng. Technol.* **2017**, *12*, 2333–2341.
21. Wang, Q.; Rafiq, M.; Lv, Y.Z.; Li, C.R.; Yi, K. Preparation of Three Types of Transformer Oil-based Nanofluids and Comparative Study on the Effect of Nanoparticle Concentrations on Insulating Property of Transformer Oil. *J. Nanotechnol.* **2016**, *2016*, 5802753. [[CrossRef](#)]
22. Peppas, G.D.; Bakandritsos, A.; Charalampakos, V.P.; Pyrqiotti, E.C.; Tucek, J.; Zboril, R.; Gonos, I.F. Ultrastable Natural Ester-based Nanofluids for High Voltage Insulation Applications. *ACS Appl. Mater. Interfaces* **2016**, *8*, 25202–25209. [[CrossRef](#)]

23. Du, Y.F.; Lv, Y.Z.; Li, C.; Chen, M.; Zhou, J.; Li, X.X.; Zhou, Y.; Tu, Y. Effect of Electron Shallow Trap on Breakdown Performance of Transformer Oil-based Nanofluids. *J. Appl. Phys.* **2011**, *110*, 104104. [[CrossRef](#)]
24. Zhong, Y.; Lv, Y.; Li, C.; Du, Y.; Chen, M.; Zhang, S.; Zhou, Y.; Chen, L. Insulating Properties and Charge Characteristics of Natural Ester Fluid Modified by TiO₂ Semiconductive Nanoparticles. *IEEE Trans. Dielectr. Electr. Insul.* **2013**, *20*, 135–140. [[CrossRef](#)]
25. Saenkhumwong, W.; Suksri, A. The Improved Dielectric Properties of Natural Ester Oil by using ZnO and TiO₂ Nanoparticles. *Eng. Appl. Sci. Res.* **2017**, *44*, 148–153.
26. Nor, S.F.M.; Azis, N.; Jasni, J.; Ab Kadir, M.Z.A.; Yunus, R.; Yaakub, Z. Investigation on the Electrical Properties of Palm Oil and Coconut Oil based TiO₂ Nanofluids. *IEEE Trans. Dielectr. Electr. Insul.* **2017**, *24*, 3432–3442. [[CrossRef](#)]
27. Mansour, D.-E.A.; Elsaheed, A.M.; Izzularab, M.A. The Role of Interfacial Zone in Dielectric Properties of Transformer Oil-based Nanofluids. *IEEE Trans. Dielectr. Electr. Insul.* **2016**, *23*, 3364–3372. [[CrossRef](#)]
28. Huifei, J.; Andritsch, T.; Tsekmes, I.A.; Kochetov, R.; Morshuis, P.H.F.; Smit, J.J. Properties of Mineral Oil based Silica Nanofluids. *IEEE Trans. Dielectr. Electr. Insul.* **2014**, *21*, 1100–1108. [[CrossRef](#)]
29. Prasad, D.; Chandrasekar, S. Investigations on Dielectric Performance Characteristics of Natural Ester based Nano-fluids for Power Transformer Applications. *Asian J. Res. Soc. Sci. Humanit.* **2016**, *6*, 1146–1157. [[CrossRef](#)]
30. Dong, M.; Dai, J.; Li, Y.; Xie, J.; Ren, M.; Dang, Z. Insight into the Dielectric Response of Transformer Oil-based Nanofluids. *AIP Adv.* **2017**, *7*, 025307. [[CrossRef](#)]
31. Fontes, D.H.; Ribatski, G.; Filho, E.P.B. Experimental Evaluation of Thermal Conductivity, Viscosity and Breakdown Voltage AC of Nanofluids of Carbon Nanotubes and Diamond in Transformer Oil. *Diam. Relat. Mater.* **2015**, *58*, 115–121. [[CrossRef](#)]
32. Liu, D.; Zhou, Y.; Yang, Y.; Zhang, L.; Jin, F. Characterization of High Performance AlN Nanoparticle-based Transformer Oil Nanofluids. *IEEE Trans. Dielectr. Electr. Insul.* **2016**, *23*, 2757–2767. [[CrossRef](#)]
33. Mohamad, N.A.; Azis, N.; Jasni, J.; Yunus, R.; Ab Kadir, M.Z.A.; Yaakub, Z. Effects of Different Types of Surfactants on AC Breakdown Voltage of Refined, Bleached and Deodorized Palm Oil based CuO Nanofluids. In Proceedings of the IEEE PES Asia-Pacific Power and Energy Engineering Conference (APPEEC), Kota Kinabalu, Sabah, 7–10 October 2018; pp. 768–771.
34. Cavallini, A.; Karthik, R.; Negri, F. The Effect of Magnetite, Graphene Oxide and Silicone Oxide Nanoparticles on Dielectric Withstand Characteristics of Mineral Oil. *IEEE Trans. Dielectr. Electr. Insul.* **2015**, *22*, 2592–2600. [[CrossRef](#)]
35. Karthik, R.; Raymon, A. Effect of Silicone Oxide Nanoparticles on Dielectric Characteristics of Natural Ester. In Proceedings of the IEEE International Conference on High Voltage Engineering and Application (ICHVE), Chengdu, China, 19–22 September 2016; pp. 1–3.
36. Jin, H.; Morshuis, P.H.F.; Smit, J.J.; Andritsch, T. The Effect of Surface Treatment of Silica Nanoparticles on the Breakdown Strength of Mineral Oil. In Proceedings of the IEEE International Conference on Liquid Dielectrics (ICDL), Bled, Slovenia, 29 June–3 July 2014; pp. 1–4.
37. Lee, J.C.; Kim, W.Y. Experimental Study on the Dielectric Breakdown Voltage of the Insulating Oil Mixed with Magnetic Nanoparticles. *Phys. Procedia* **2012**, *32*, 327–334. [[CrossRef](#)]
38. Rafiq, M.; Li, C.; Ge, Y.; Lv, Y.; Yi, K. Effect of Fe₃O₄ nanoparticle concentrations on dielectric property of transformer oil. In Proceedings of the IEEE International Conference High Voltage Engineering Application (ICHVE), Chengdu, China, 19–22 September 2016; pp. 1–4.
39. ISO 5508:1990. *Animal and Vegetable Fats and Oils—Analysis by Gas Chromatography (GC) of Methyl-Esters of Fatty Acids*; International Organization for Standardization: Geneva, Switzerland, 1990.
40. Hwang, Y.; Lee, J.K.; Lee, C.H.; Jung, Y.M.; Cheong, S.I.; Lee, C.G.; Ku, B.C.; Jang, S.P. Stability and Thermal Conductivity Characteristics of Nanofluids. *Thermochim. Acta* **2007**, *455*, 70–74. [[CrossRef](#)]
41. ASTM D1816. *Standard Test Method for Dielectric Breakdown Voltage of Insulating Liquids Using VDE Electrodes*; ASTM International: West Conshohocken, PA, USA, 2012.
42. ASTM D6304. *Standard Test Method for Determination of Water in Petroleum Products, Lubricating Oils and Additives by Coulometric Karl Fisher Titration*; ASTM International: West Conshohocken, PA, USA, 2016.
43. Michal, O.; Mentlík, V.; Trnka, P.; Hornak, J.; Totzauer, P. Dielectric Properties of Biodegradable Vegetable Oil based Nanofluid. In Proceedings of the 19th International Scientific Conference on Electric Power Engineering (EPE), Brno, Czech Republic, 16–18 May 2018; pp. 1–4.

44. Du, B.; Li, J.; Yang, L.J.; Yao, W.; Yao, S. Dielectric Properties of Vegetable Oil Modified by Monodispersed Fe₃O₄ Nanoparticles. In Proceedings of the International Conference on High Voltage Engineering and Application (ICHVE), Poznan, Poland, 8–11 September 2014; pp. 4–7.
45. Karthik, R.; Raja, T.S.R.; Madavan, R. Enhancement of Critical Characteristics of Transformer Oil using Nanomaterials. *Arab. J. Sci. Eng.* **2013**, *38*, 2725–2733. [[CrossRef](#)]



© 2019 by the authors. Licensee MDPI, Basel, Switzerland. This article is an open access article distributed under the terms and conditions of the Creative Commons Attribution (CC BY) license (<http://creativecommons.org/licenses/by/4.0/>).